Analytical and Numerical Investigation for the DMBBM Equation

Abdulghani Alharbi[1], Mahmoud A. E. Abdelrahman[1, 2, *] and M. B. Almatrafi[1]

Abstract: The nonlinear dispersive modified Benjamin-Bona-Mahony (DMBBM) equation is solved numerically using adaptive moving mesh PDEs (MMPDEs) method. Indeed, the exact solution of the DMBBM equation is obtained by using the extended Jacobian elliptic function expansion method.   The current methods give a wider applicability for handling nonlinear wave equations in engineering and mathematical physics. The adaptive moving mesh method is compared with exact solution by numerical examples, where the explicit solutions are known. The numerical results verify the accuracy of the proposed method.

1 Introduction

Many important phenomena in natural science can be modelled by nonlinear partial differential equations (NLPDEs).   NLPDEs are widely used to describe complex phenomena in various sciences, especially in nonlinear optics, solid state physics, fluid mechanics, quantum mechanics, geochemistry, biology and so on, see Abdelrahman et al. [Abdelrahman and Kunik (2014, 2015); Abdelrahman (2017a,b); Abdelrahman and Sohaly (2017); Younis, Ali and Mahmood (2015); Bhrawy (2014); Dehghan, Abbaszadeh and Mohebbi (2014b, 2015a)].   Therefore, the study of the travelling wave solutions for NLPDEs plays an important role in the study of nonlinear science. Recently, many powerful mathematical techniques, such as tanh-sech method [Malflieta and Hereman (1996); Wazwaz (2004b)], Jacobi elliptic function method [Dai and Zhang (2006); Liu, Fu, Liu et al. (2001)], $(\frac{G'}{G})-$ expansion method [Wang, Zhang and Li (2008); Zhang, Tong and Wang (2008)], exp-function method [He and Wu (2006); Aminikhad, Moosaei and Hajipour (2009)], homotopy analysis method [Liao (2005)], sine-cosine method [Wazwaz (2005, 2004a)], homogeneous balance method [Fan and Zhang (1998); Wang (1996)], F-expansion

[1]Department of Mathematics, College of Science, Taibah University, Al-Madinah Al-Munawarah, Saudi Arabia.

[2]Department of Mathematics, Faculty of Science, Mansoura University, Mansoura, Egypt.

*Corresponding Author: Mahmoud A. E. Abdelrahman.

 Email: mahmoud.abdelrahman@mans.edu.eg; maabdelrahman@taibahu.edu.sa.

method [Ren and Zhang (2006); Zhang, Wang, Wang et al. (2006)], extended tanh-method [Fan (2000); Wazwaz (2007)], Riccati-Bernoulli sub-ODE method [Yang, Deng and Wei (2005); Abdelrahman and Sohaly (2018)], modified trial equation method [Bulut, Yel and Baskonus (2017); Kocak, Bulut and Yel (2014)] and so on, have been proposed for obtaining exact solutions to the NLPDEs.

This paper is concerned with the (1+1)-dimensional nonlinear dispersive modified Benjamin-Bona-Mahony (DMBBM) equation [Yusufoglu (2008)], in the form

$$u_t + u_x - \alpha u^2 u_x + u_{xxx} = 0, \tag{1}$$

where α is a non-zero constant. This equation describes an approximation for surface long waves in nonlinear dispersive media. Moreover, it characterizes the hydro magnetic waves in cold plasma, acoustic gravity waves in compressible fluids and acoustic waves in inharmonic crystals [Yusufoglu (2008); Khan, Akbar and Islam (2014)].

We obtain the numerical solution of PDEs by approximating the PDEs on a mesh. We divide the domain into a finite set of nodes to obtain a uniform mesh. It is well known that some solutions have regions with rapid variations such as steep fronts, shock-like structures. To resolve this kind of region, we need to use a massive number of points, which means the step size, $h = x_i - x_{i-1}$, should be small enough for the entire domain. Computationally, this is intensive and expensive. Therefore, we attempt to find an alternative approach to have an adaptive mesh that manually puts more points in regions in which the solution changes rapidly and fewer points elsewhere. Unfortunately, this is useful only in time-independent problems. So, if the solution moves as the time moves, we must redistribute the mesh in each time. Overcoming this kind of issue, we use the adaptive moving mesh methods, which focus on the regions with rapid variations and moves the mesh as the solution moves with time. The adaptive mesh intends to have an adequate quality of accuracy and efficiency without using an excessive number of mesh points, as compared to a different method such as uniform mesh method.

Dehghan et al. [Dehghan, Abbaszadeh and Mohebbi (2015b)] solved the two-dimensional nonlinear generalized Benjamin-Bona-Mahony-Burgers, using interpolating element-free Galerkin technique. Indeed, Dehghan et al. [Dehghan, Abbaszadeh and Mohebbi (2014a)] considered the three-dimensional nonlinear generalized Benjamin-Bona-Mahony-Burgers equation equation via the meshless method of radial basis functions. The results given in Dehghan et al. [Dehghan, Abbaszadeh and Mohebbi (2015b, 2014a)] are so efficient and robust. In this paper, we apply the extended Jacobian elliptic function expansion method [Chen, Xu, Liu et al. (2003)] to construct the exact solutions for the (1+1)-dimensional nonlinear dispersive modified Benjamin-Bona-Mahony (DMBBM) equation. The numerical part of this article will be investigated by using the r-adaptive moving mesh method [Huang and Russell (2010); Budd, Huang and Russell (2009); Liseikin (2009)], which works with a monitor function, sometimes referred to as a mesh density function, and moving mesh partial differential equations (MMPDEs). The procedure of this method is embodied in moving a fixed number of grid nodes into regions in which the error of the solution is high. The monitor function fluctuates/moves according

to the movement of a particular solution, such as a solution with large curvatures. On other words, the mesh density function is distributed between the grid elements. It is important to mention that an appropriate selection for the monitor function powerfully contributes to a great performance of this method. Since the r-adaptive moving mesh method refines the mesh, the internal layers are resolved more accurately. It is notable to notice that the MMPDEs can be rewritten by a diffusion equation [Huang and Russell (2010); Budd, Huang and Russell (2009)]. As a result, the MMPDEs can be simply executed within the finite difference techniques. A massive number of natural problems (for instance, problems occurred in fluid mechanics [Tang (2005); Yibao, Jeong and Kim (2014)], heat transfer [Ceniceros and Hou (2001)] and meteorological [Walsh (2010); Budd, Cullen and Walsh (2013)]) has been successfully solved by applying the r-adaptive techniques.

The organization of this article is given as follows. In Section 2, we give some new exact solutions to the DMBBM equation, using extended Jacobian elliptic function expansion method. In Section 3, we introduce the numerical solution for the DMBBM equation, namely on a fixed mesh or on an adaptive mesh. Moreover, we give a comparison between exact and numerical solutions. Section 4 is devoted to conclude this work.

2 The extended Jacobian elliptic function expansion method

Using the traveling wave transformation

$$u(x,t) = u(\xi), \qquad \xi = x - \mu t, \tag{2}$$

where μ is a real constant, Eq. (1) transforms into the following ODEs:

$$u''' + (1-\mu)u' - \alpha u^2 u' = 0. \tag{3}$$

Integrating with respect to ξ and taking the constant of the integration by zero, we obtain the following ODE:

$$3u'' - \alpha u^3 + 3(1-\mu)u = 0. \tag{4}$$

According to the extended Jacobian elliptic function expansion method [Chen, Xu, Liu et al. (2003)], the solution of Eq. (4) can be expressed in the following form:

$$u = a_0 + a_1 sn(\xi, m) + b_1 cn(\xi, m), \tag{5}$$

where a_0, a_1 and b_1 are constants determined later. From Eq. (5) we have

$$u' = a_1 cn(\xi)\, dn(\xi, m) - b_1 sn(\xi, m)\, dn(\xi, m), \tag{6}$$

$$u'' = -m^2 sn(\xi, m)\, a_1 + 2\, a_1 sn(\xi, m)^3 m^2 + 2\, m^2 sn(\xi, m)^2 cn(\xi, m)\, b_1 - a_1 sn(\xi, m) - b_1 cn(\xi, m). \tag{7}$$

Substituting Eqs. (5)-(7) into Eq. (4) and equating all the coefficients of sn^3, $sn^2 cn$, sn^2, $sncn$, sn, cn, sn^0 to zero, we obtain that:

$$6m^2 a_1 - \alpha\left(a_1^3 - 3\, a_1 b_1^2\right) = 0, \tag{8}$$

$$6\, m^2 b_1 - \alpha\left(3\, a_1^2 b_1 - b_1^3\right) = 0, \tag{9}$$

$$a_0 \left(a_1^2 - b_1^2 \right) = 0, \tag{10}$$

$$a_0 a_1 b_1 = 0, \tag{11}$$

$$-3a_1 \, m^2 - \alpha \left(3 \, a_0^2 a_1 + 3 \, a_1 b_1{}^2 \right) - 3 \, \mu \, a_1 = 0, \tag{12}$$

$$\alpha \left(3 \, a_0^2 b_1 + b_1^3 \right) + 3 \, \mu \, b_1 = 0, \tag{13}$$

$$-\alpha \left(a_0^3 + 3 \, a_0 b_1^2 \right) + 3(1 - \mu) a_0 = 0. \tag{14}$$

Solving the above system of equations yields the following cases:

Case 1.

$a_0 = 0, \ a_1 = 0, \ b_1 = \pm \sqrt{\frac{6}{\alpha}} \, m \, i, \ \mu = 2m^2.$

Then, the first family of equation is

$$u_1(x, t) = \pm \sqrt{\frac{6}{\alpha}} \, m \, i \, cn(x - \mu t). \tag{15}$$

As long as $m \to 1$, Eq. (15) is degenerated as follows:

$$u_1(x, t) = \pm \sqrt{\frac{6}{\alpha}} \, i \, sech(x - 2t). \tag{16}$$

Case 2.

$a_0 = 0, a_1 = \pm \sqrt{\frac{3}{2\alpha}} \, m, b_1 = -\sqrt{\frac{3}{2\alpha}} \, m \, i, \mu = \frac{m^2}{2}.$

Then, the second family of equation is

$$u_2(x, t) = \pm \sqrt{\frac{3}{2\alpha}} \, m \, sn(x - \mu t) - \sqrt{\frac{3}{2\alpha}} \, m \, i \, cn(x - \mu t). \tag{17}$$

As long as $m \to 1$, Eq. (19) is degenerated on the following form:

$$u_2(x, t) = \pm \sqrt{\frac{3}{2\alpha}} \, tanh(x - \frac{1}{2}t) - i \sqrt{\frac{3}{2\alpha}} \, m \, sech(x - \frac{1}{2}t). \tag{18}$$

Case 3.

$a_0 = 0, a_1 = \pm \sqrt{\frac{3}{2\alpha}} \, m, b_1 = \sqrt{\frac{3}{2\alpha}} \, m \, i, \mu = \frac{m^2}{2}.$

Then, the second family of equation is

$$u_3(x, t) = \pm \sqrt{\frac{3}{2\alpha}} \, m \, sn(x - \mu t) + \sqrt{\frac{3}{2\alpha}} \, m \, i \, cn(x - \mu t). \tag{19}$$

As long as $m \to 1$, Eq. (19) is degenerated as the following form:

$$u_3(x, t) = \pm \sqrt{\frac{3}{2\alpha}} \, tanh(x - \frac{1}{2}t) + i \sqrt{\frac{3}{2\alpha}} \, sech(x - \frac{1}{2}t). \tag{20}$$

Case 4.

$a_0 = 0, a_1 = \pm \sqrt{\frac{6}{\alpha}} \, m, b_1 = 0, \mu = -m^2.$

Then, the fourth family of equation is

$$u_4(x,t) = \pm\sqrt{\frac{6}{\alpha}}\, m\, sn(x - \mu t). \tag{21}$$

As long as $m \to 1$, Eq. (21) is degenerated as follows:

$$u_4(x,t) = \pm\sqrt{\frac{6}{\alpha}}\, tanh(x + t). \tag{22}$$

3 Numerical results

This section is mainly devoted to seek the numerical solution of Eq. (1), where $(x,t) \in [a,b] \times [0,T_e]$. Here, a and b are supposed to be the boundaries of the spatial domain and T_e denotes a particular time. As mentioned previously, the adaptive moving mesh and fixed mesh techniques are employed to obtain the numerical results of Eq. (1). The corresponding boundary conditions used in these methods are given as follows:

$$u_x(a,t) = u_{xxx}(a,t) = 0, \qquad u_x(b,t) = u_{xxx}(b,t) = 0, \quad \forall\, t \in [0,T_e]. \tag{23}$$

Furthermore, the corresponding initial condition is selected by calculating the exact solution (Eq. (22)) at $t = 0$.

3.1 Numerical results of Eq. (1) on a fixed mesh

The physical domain is uniformly partitioned into $N + 1$ points by assuming that

$$x_i = (i - 1)h, \quad x_i \in [a,b], \quad 1 \le i \le N + 1,$$

where $h = (b - a)/N$. We also use the centred finite differences so as to discretise the derivatives appeared in Eq. (1) as follows:

$$u_{t,i} = -\frac{f_{i+1} - f_i}{h},$$
$$f_i = \frac{u_{i+1} - 2u_i + u_{i-1}}{h^2} + u_{i+\frac{1}{2}} - \frac{\alpha}{3}u_{i+\frac{1}{2}}^3, \tag{24}$$

where $u_{i+\frac{1}{2}} = 0.5(u_{i+1} + u_i)$, $u_{i+\frac{1}{2}}^3 = 0.5(u_{i+1}^3 + u_i^3)$ and $i = 2, ..., N$. The boundary conditions presented in Eq. (23) are replaced with $u_{t,1} = 0$ and $u_{t,N+1} = 0$, and the initial condition is selected by evaluating Eq. (22) at $t = 0$.

Fig. 1 illustrates how the uniform solution evolves with time. The parameters are taken to be $\alpha = 3$, $\mu = 1$, $a = -10$, $b = 10$, $N = 1000$ and t is taken between $t = 0$ to $t = 5$. Notice that the solution travels as the time progresses and does not evolve as can be observed in this figure. It can be also noted that the numerical solution (solid green line), at $t = 5$, is roughly identical to the exact solution (blue dashed line) obtained using Eq. (22) at $t = 5$.
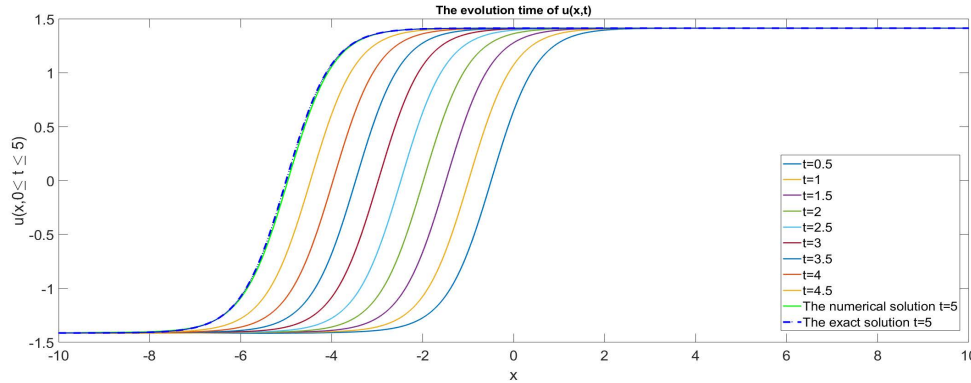
Figure 1: Showing the time evolution of $u(x,t)$ applying the scheme Eq. (24). The parameter values are taken to be $\alpha = 3$, $\mu = -1$, $a = -10$, $b = 10$, $N = 1000$ and t is taken between $t = 0$ to $t = 5$

3.2 Numerical results of Eq. (1) on an adaptive mesh

This subsection mostly focuses on finding the numerical results of Eq. (1) by employing the adaptive moving mesh methods. The coordinate transformation is taken by

$x = x(\xi, t) \colon [0,1] \to [a,b], \ t > 0,$

where x and ξ are assumed to be the spatial and computational coordinates, respectively. Consequently, the solution u is obviously represented as follows:

$$u(x,t) = u(x(\xi,t),t). \tag{25}$$

Hence, the moving mesh which is related to the solution appeared in Eq. (25) is illustrated by $\mathcal{J}_h(ts) \colon x_i(\xi) = x(\xi_i, t), \ i = 1, \cdots, N+1$, and the end points of the physical domain are described by $x_1 = a, \quad x_{N+1} = b$. Further, the regular grid evaluated on the computational domain is shown as follows: $\mathcal{J}_h^c(t) \colon \xi_i = (i-1)/N, \ i = 1, \cdots, N+1$. Applying the chain rule to Eq. (1) yields

$$
\begin{aligned}
u_{t,i} - \frac{u_{i+1} - u_{i-1}}{x_{i+1} - x_{i-1}} x_t &= \frac{-2}{x_{i+1} - x_{i-1}} (f_i - f_{i-1}), \\
f_i &= \frac{2}{x_{i+1} - x_{i-1}} \left(\frac{f_{i+1} - f_i}{x_{i+1} - x_i} - \frac{f_i - f_{i-1}}{x_i - x_{i-1}} \right) + u_{i+\frac{1}{2}} - \frac{\alpha}{3} u_{i+\frac{1}{2}}^3,
\end{aligned} \tag{26}
$$

where $u_{i+\frac{1}{2}} = 0.5(u_{i+1} + u_i)$, $u_{i+\frac{1}{2}}^3 = 0.5(u_{i+1}^3 + u_i^3)$ and $i = 2, ..., N$. The boundary conditions presented in Eq. (23) are replaced with $u_{t,1} = 0$ and $u_{t,N+1} = 0$, and the initial condition is selected by evaluating Eq. (22) at $t = 0$. It should be pointed out that the coordinate transformation $x(\xi)$ is obtained by utilizing the MMPDEs and the MMPDE7 whose semi-discretisation is given by ([Alharbi and Naire (2017, 2019); Alharbi (2016)])

$$\text{MMPDE7:} \quad x_{t,i} = \frac{1}{2h^2 \tau q_i} ((x_{i+1} - x_i)(q_{i+1} + q_i) - (x_i - x_{i-1})(q_i + q_{i-1})), \tag{27}$$

Table 1: Presenting the errors, measured using L_2 norm, and CPU time taken for both the uniform mesh and adaptive mesh schemes. We used, here, MMPDE7 and the arc-length monitor function. The parameters are given by $\alpha = 3$, $\mu = -1$, $a = -10$, $b = 10$, $\tau = 10^{-2}$ and $\lambda = 5$

N (Δx)	Measured Error (L_2 norm)		CPU time taken to reach $t = 5$	
	Uniform mesh	Adaptive moving mesh	Uniform mesh	Adaptive moving mesh
200 (0.1)	1.5×10^{-2}	2.8×10^{-4}	2.3×10^{-1} s	4×10^{-1} s
400 (0.05)	7.8×10^{-3}	6.7×10^{-5}	5.5×10^{-1} s	7×10^{-1} s
800 (0.025)	3.9×10^{-3}	1.66×10^{-5}	9×10^{-1} s	1.28 s
1600 (0.0125)	2×10^{-3}	4.13×10^{-6}	1.65 s	3.06 s
3200 (0.00625)	9.9×10^{-4}	1.03×10^{-6}	5.07 s	8.56 s
6400 (0.003125)	4.9×10^{-4}	2.56×10^{-7}	14.4 s	20 s
8000 (0.0025)	3.9×10^{-4}	1.63×10^{-7}	16.5 s	42.56 s
10000 (0.002)	3.1×10^{-4}	1.05×10^{-7}	28.7 s	85.9 s

is also employed in this subsection. $q(x, t)$ represents the mesh density function and τ is a constant. The boundary conditions are given by $x_{t,1} = 0$ and $x_{t,N+1} = 0$. In addition, the initial condition of the mesh is chosen by $x(\xi, 0) = (i - 1)h$, $i = 1, 2, \ldots, N + 1$, where $h = (b - a)/N$. The mesh density function is chosen as follows:

Arc-length monitor function :$\quad q_i(x, u) = \sqrt{1 + \lambda \left(\dfrac{u_{i+1} - u_{i-1}}{x_{i+1} - x_{i-1}} \right)^2}$, $\qquad$ (28)

where λ is considered to be a non-negative constant. Several forms of smoothing to the mesh density function are used so as to support the uniform grid [Tang (2005); Ceniceros and Hou (2001); Huang (2001)]. If the solution is not smooth enough, then the computed monitor function can often cause a sudden change and make the computation stiffer. In order to have a smoother mesh and make the mesh equation simpler to integrate, we use a smoothing scheme such as the weighted averaging scheme proposed by Huang et al. [Huang and Russell (2010)]. This scheme is formed as

$\hat{q}_i = 0.25q_{i-1} + 0.5q_i + 0.25q_{i+1}$,
$\hat{q}_1 = 0.5 \left(q_1 + q_2 \right)$, $\qquad$ (29)
$\hat{q}_{N+1} = 0.5 \left(q_N + q_{N+1} \right)$.

The considered parameters are taken by $\alpha = 3$, $\mu = -1$, $a = -10$, $b = 10$, $\tau = 10^{-2}$ and $\lambda = 5$. Eventually, we compare the schemes in terms of accuracy and convergence. To do that, we obtain the exact solution (Eq. (22)) and the numerical results to both the uniform and the adaptive mesh schemes at $t = 5$.

Figs. 2(a)-2(c) present the time evolution of $u(x, t)$, $x(\xi, t)$, and $\hat{q}(x, t)$, respectively, using the adaptive moving mesh with MMPDE7 Eq. (27) and the arc-length monitor function
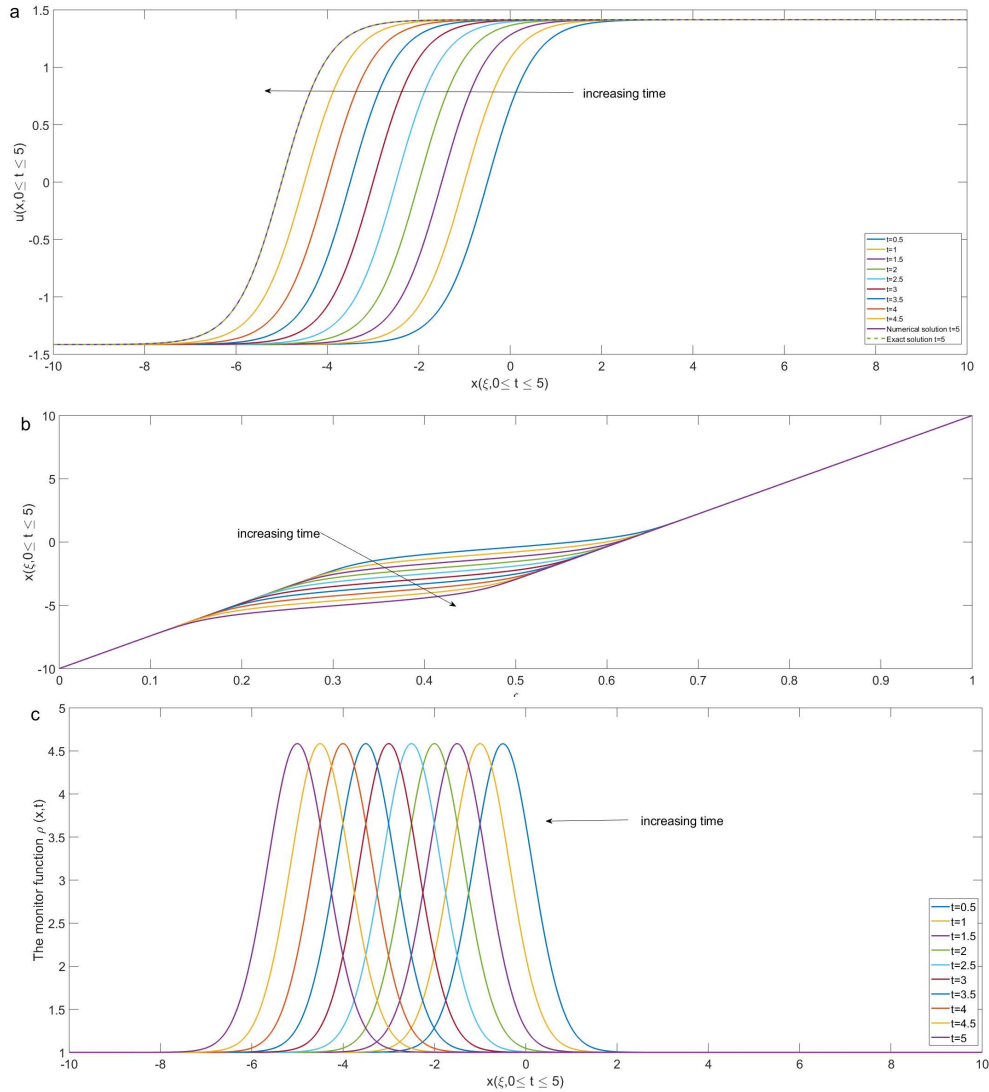
Figure 2: (a, b, c) The time evolution of $u(x, t)$, $x(\xi, t)$, and $\hat{q}(x, t)$, respectively, using the adaptive moving mesh with MMPDE7 Eq. (27) and the arc-length monitor function Eq. (28). The parameter values are $\alpha = 3$, $\mu = -1$, $a = -10$, $b = 10$, $\tau = 10^{-2}$ and $\lambda = 5$
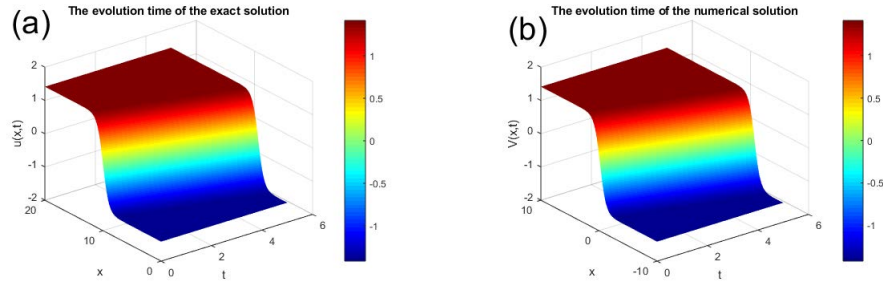
Figure 3: (a, b) show the time evolution of both the exact solution to Eq. (16) and the numerical solution, respectively. We use the adaptive moving mesh scheme with the arc-length monitor function Eq. (28) and MMPDE7 Eq. (27). Time is taken between $t = 0$ to $t = 5$. The parameter values used here are $\alpha = 3$, $\mu = -1$, $a = -10$, $b = 10$, $\tau = 10^{-2}$ and $\lambda = 5$
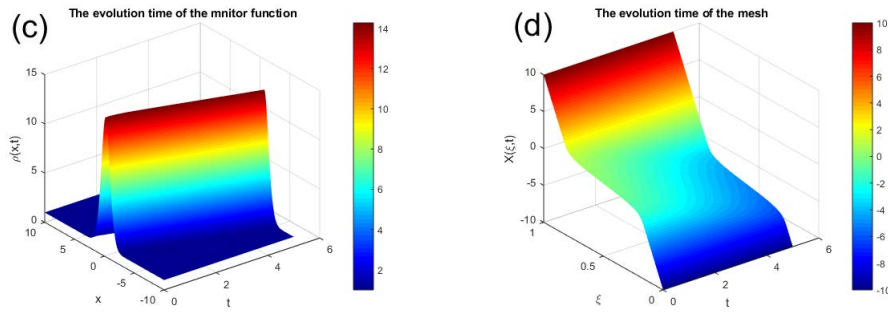

Figure 4: (c, d) illustrate the time evolution of both the adaptive mesh obtained by applying MMPDE7 Eq. (27) and the arc-length monitor function Eq. (28), respectively, where $t = 0 \to 5$

Eq. (28). The parameter values are taken by $\alpha = 3$, $\mu = -1$, $a = -10$, $b = 10$. The parameter of the MMPDE7 and the constant of the arc-length monitor function are chosen by $\tau = 10^{-2}$ and $\lambda = 5$, respectively. From Fig. 2(b), we observe that the mesh concentrates and moves to the steep front ahead and behind it. Fig. 2(b) shows the arc-length monitor function related to the changes in the solution, where large values of the monitor function result in the rose number of grids re-distributed in the steep front region.

Figs. 3(a) and 3(b) display the time evolution of both the exact solution to Eq. (22) and the numerical solution, respectively. We use the adaptive moving mesh scheme Eq. (26) with the arc-length monitor function Eq. (28) and MMPDE7 Eq. (27), where $t = 0 \to 5$. The parameters values are given as follows: $\alpha = 3$, $\mu = -1$, $a = -10$ and $b = 10$. The parameter of MMPDE7 and the associated constant of the arc-length monitor function are taken by $\tau = 10^{-2}$ and $\lambda = 5$, respectively. It can be simply observed that the numerical and exact solutions are roughly identical. Figs. 4(c) and 4(d) show the time evolution of both the adaptive mesh obtained by applying MMPDE7 Eq. (27) and the arc-length monitor
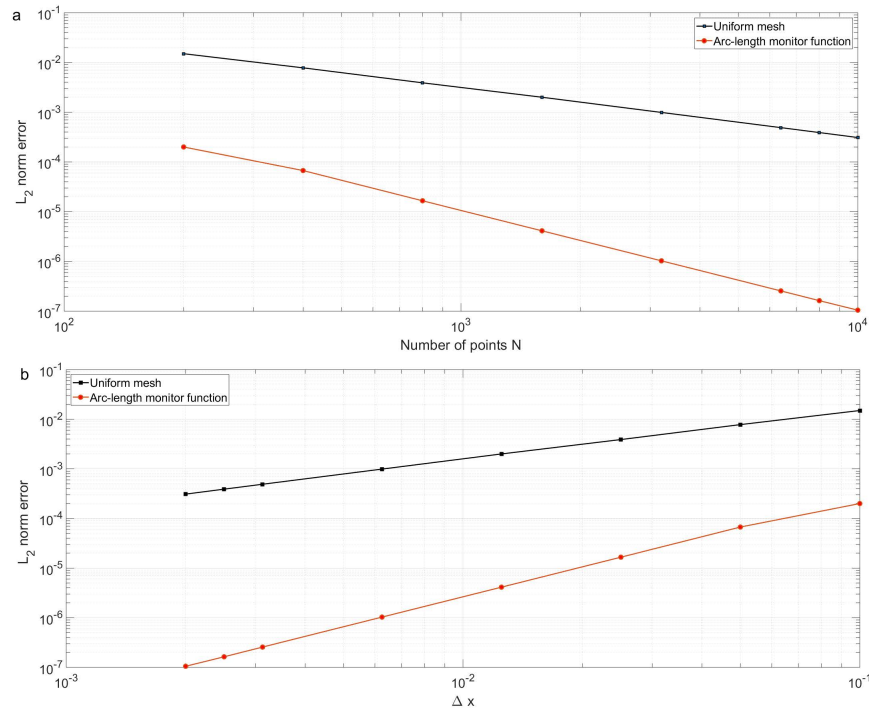
Figure 5: (a, b) show a summary of the errors' columns presented in Tab. (1)

function Eq. (28), respectively. Time is chosen to move between 0 and 5. Remark that the monitor function, appeared in Fig. 4(c), takes 1 everywhere except the area of the steep front. Therefore, it controls the movement of the mesh points, illustrated in Fig. 4(d), so that the region of the steep front takes more points than elsewhere.

Tab. 1 presents how the numerical solutions obtained using the above schemes are convergent to the exact solution. The error is measured by obtaining the numerical results for above schemes at $t = 5$. Figs. 5(a) and 5(b) demonstrate a brief description of the errors' columns, presented in Tab. 1. Notice that the adaptive moving mesh solution is outstandingly accurate and concurrent to the exact solution than that obtained using the uniform mesh scheme. For the CPU time taken, the uniform mesh and adaptive moving mesh schemes take a very similar time to arrive at $t = 5$ for the same value of Δx. Finally, we can surely assume that the technique of the adaptive moving mesh is more accurate and convergent than that of the uniform mesh scheme.

4 Conclusions

In this article, we have solved the DMBBM equation numerically using adaptive moving mesh PDEs (MMPDEs) method. Moreover, it has shown that the extended Jacobian elliptic function expansion technique can be used for building the wave solutions for the DMBBM equation. The main advantage of this method is that it gives results in terms of the Jacobi elliptic function which are more general. Indeed, these solutions may have

significant applications in physics and applied mathematics. The comparison between the exact and numerical solutions are also investigated. The results of this work show how the adaptive moving mesh PDEs (MMPDEs) method is very powerful, robust and vital. Another interesting aspect of these results is that the proposed two methods used can be applied to other nonlinear equation in applied science.

Acknowledgment: The authors want to thank the editor and reviewers for valuable comments.

Conflicts of Interest: The authors declare that they have no conflicts of interest to report regarding the present study.

References

Abdelrahman, M. A. E. (2017): Global solutions for the ultra-relativistic Euler equations. *Nonlinear Analysis*, vol. 155, pp. 140-162.

Abdelrahman, M. A. E. (2017): On the shallow water equations. *Zeitschrift für Naturforschung A*, vol. 72, no. 9, pp. 873-879.

Abdelrahman, M. A. E.; Kunik, M. (2014): The interaction of waves for the ultra-relativistic Euler equations. *Journal of Mathematical Analysis and Applications*, vol. 409, pp. 1140-1158.

Abdelrahman, M. A. E.; Kunik, M. (2015): The ultra-relativistic Euler equations. *Mathematical Methods in the Applied Sciences*, vol. 38, pp. 1247-1264.

Abdelrahman, M. A. E.; Sohaly, M. A. (2017): Solitary waves for the nonlinear Schrödinger problem with theprobability distribution function in the stochastic input case. *The European Physical Journal Plus*, vol. 132, no. 8, pp. 339.

Abdelrahman, M. A. E.; Sohaly, M. A. (2019): On the new wave solutions to the MCH equation. *Indian Journal of Physics*, vol. 93, no. 7, pp. 903-911.

Alharbi, A. R. (2016): *Numerical Solution of Thin-Film Flow Equations Using Adaptive Moving Mesh Methods (Ph.D. Thesis)*. Keele University.

Alharbi, A. R.; Naire, S. (2017): An adaptive moving mesh method for thin film flow equations with surface tension. *Journal of Computational and Applied Mathematics*, vol. 319, no. 4, pp. 365-384.

Alharbi, A. R.; Naire, S. (2019): An adaptive moving mesh method for two-dimensional thin film flow equations with surface tension. *Journal of Computational and Applied Mathematics*, vol. 356, pp. 219-230.

Aminikhad, H.; Moosaei, H.; Hajipour, M. (2009): Exact solutions for nonlinear partial differential equations via Exp-function method. *Numerical Methods for Partial Differential Equations*, vol. 26, pp. 1427-1433.

Bhrawy, A. H. (2014): An efficient Jacobi pseudospectral approximation for nonlinear complex generalized Zakharov system. *Applied Mathematics and Computation*, vol. 247, pp. 30-46.

Budd, C. J.; Cullen, M. J. P.; Walsh, E. J. (2013): Monge-Ampère based moving mesh methods for numerical weather prediction, with applications to the Eady problem. *Journal of Computational Physics*, vol. 236, pp. 247-270.

Budd, C. J.; Huang, W.; Russell, R. D. (2009): Adaptivity with moving grids. *Acta Numerica*, vol. 18, pp. 111-241.

Bulut, H.; Yel, G.; Baskonus, H. M. (2017): Novel structure to the coupled nonlinear Maccari's system by using modified trial equation. *Advanced Mathematical Models & Applications*, vol. 2, no. 1, pp. 14-19.

Ceniceros, H. D.; Hou, T. Y. (2001): An efficient dynamically adaptive mesh for potentially singular solutions. *Journal of Computational Physics*, vol. 172, no. 2, pp. 609-639.

Chen, L.; Xu, Y.; Liu, Z. F.; Han, J. H. (2003): The extended jacobian elliptic function expansion method and its application to nonlinear wave equation. *FIZIKA A-ZAGREB-*, vol. 12, no. 4, pp. 161-170.

Dai, C. Q.; Zhang, J. F. (2006): Jacobian elliptic function method for nonlinear differential difference equations. *Chaos Solutions Fractals*, vol. 27, pp. 1042-1049.

Dehghan, M.; Abbaszadeh, M.; Mohebbi, A. (2014): The numerical solution of nonlinear high dimensional generalized Benjamin-Bona-Mahony-Burgers equation via the meshless method of radial basis functions. *Computers & Mathematics with Applications*, vol. 68, no. 3, pp. 212-237.

Dehghan, M.; Abbaszadeh, M.; Mohebbi, A. (2014): Numerical solution of system of N-coupled nonlinear Schrodinger equations via two variants of the meshless local Petrov Galerkin (MLPG) method. *Computer Modeling in Engineering & Sciences*, vol. 100, pp. 399-444.

Dehghan, M.; Abbaszadeh, M.; Mohebbi, A. (2015): Meshless local Petrov-Galerkin and RBFs collocation methods for solving 2D fractional klein-kramers dynamics equation on irregular domains. *CMES-Computer Modeling in Engineering & Sciences*, vol. 107, no. 6, pp. 481-516.

Dehghan, M.; Abbaszadeh, M.; Mohebbi, A. (2015): The use of interpolating element-free Galerkin technique for solving 2D generalized Benjamain-Bona-Mahony-Burgers and regularized long-wave equations on non-rectangular domains. *Journal of Computational and Applied Mathematics*, vol. 286, pp. 211-231.

Fan, E. (2000): Extended tanh-function method and its applications to nonlinear equations. *Physics Letters A*, vol. 277, pp. 212-218.

Fan, E.; Zhang, H. (1998): A note on the homogeneous balance method. *Physics Letters A*, vol. 246, pp. 403-406.

He, J. H.; Wu, X. H. (2006): Exp-function method for nonlinear wave equations. *Chaos Solitons Fractals*, vol. 30, pp. 700-708.

Huang, W. (2001): Practical aspects of formulation and solution of moving mesh partial differential equations. *Journal of Computational Physics*, vol. 171, pp. 753-775.

Huang, W.; Russell, R. D. (2010): *The Adaptive Moving Mesh Methods*. Springer.

Khan, K.; Akbar, M. A.; Islam, S. R. (2014): Exact solutions for (1+1)-dimensional nonlinear dispersive modified Benjamain-Bona-Mahony equation and coupled Klein-Gordon equations. *SpringerPlus*, vol. 3, pp. 724.

Kocak, Z. F.; Bulut, H.; Yel, G. (2014): The solution of fractional wave equation by using modified trial equation method and homotopy analysis method. *AIP Conference Proceedings*, vol. 1637, pp. 504-512.

Liao, S. (2005): Comparison between the homotopy analysis method and homotopy perturbation method. *Applied Mathematics and Computation*, vol. 169, no. 2, pp. 1186-1194.

Liseikin, V. D. (2009): *Grid Generation Methods*. Springer: New York, NY, USA.

Liu, S.; Fu, Z.; Liu, S.; Zhao, Q. (2001): Jacobi elliptic function expansion method and periodic wave solutions of nonlinear wave equations. *Physics Letters A*, vol. 289, pp. 69-74.

Malflieta, W.; Hereman, W. (1996): The tanh method: exact solutions of nonlinear evolution and wave equations. *Physica Scripta*, vol. 54, no. 6, pp. 563-568.

Ren, Y. J.; Zhang, H. Q. (2006): A generalized F-expansion method to find abundant families of Jacobi elliptic function solutions of the (2+1)-dimensional Nizhnik-Novikov-Veselov equation. *Chaos Solitons Fractals*, vol. 27, pp. 959-979.

Tang, T. (2005): Moving mesh methods for computational fluid dynamics. *Contemporary Mathematics*, vol. 383, pp. 141-173.

Walsh, E. (2010): *Moving Mesh Methods For Problems In Meteorology (Ph.D. Thesis)*. University of Bath.

Wang, M. L. (1996): Exct solutions for a compound KdV-Burgers equation. *Physics Letters A*, vol. 213, pp. 279-287.

Wang, M. L.; Zhang, J. L.; Li, X. Z. (2008): The $(\frac{G'}{G})$- expansion method and travelling wave solutions of nonlinear evolutions equations in mathematical physics. *Physics Letters A*, vol. 372, pp. 417-423.

Wazwaz, A. M. (2004): A sine-cosine method for handling nonlinear wave equations. *Mathematical and Computer Modelling*, vol. 40, pp. 499-508.

Wazwaz, A. M. (2004): The tanh method for travelling wave solutions of nonlinear equations. *Applied Mathematics and Computation*, vol. 154, no. 3, pp. 714-723.

Wazwaz, A. M. (2005): Exact solutions to the double sinh-Gordon equation by the tanh method and a variable separated ODE method. *Computers & Mathematics with Applications*, vol. 50, pp. 1685-1696.

Wazwaz, A. M. (2007): The extended tanh method for abundant solitary wave solutions of nonlinear wave equations. *Applied Mathematics and Computation*, vol. 187, pp. 1131-1142.

Yang, X. F.; Deng, Z. C.; Wei, Y. (2005): A Riccati-Bernoulli sub-ODE method for nonlinear partial differential equations and its application. *Advances in Difference Equations*, vol. 1, pp. 117-133.

Yibao, L.; Jeong, D.; Kim, J. (2014): Adaptive mesh refinement for simulation of thin film flows. *Meccanica*, vol. 49, pp. 239-252.

Younis, M.; Ali, S.; Mahmood, S. A. (2015): Solitons for compound KdV Burgers equation with variable coefficients and power law nonlinearity. *Nonlinear Dynamics*, vol. 81, pp. 1191-1196.

Yusufoglu, E. (2008): New solitary solutions for the MBBM equations using Exp-function method. *Physics Letters A*, vol. 372, pp. 442-446.

Zhang, J. L.; Wang, M. L.; Wang, Y. M.; Fang, Z. D. (2006): The improved F-expansion method and its applications. *Physics Letters A*, vol. 350, pp. 103-109.

Zhang, S.; Tong, J. L.; Wang, W. A. (2008): Generalized $(\frac{G'}{G})$- expansion method for the mKdv equation with variable coefficients. *Physics Letters A*, vol. 372, pp. 2254-2257.